Florence, Italy 12-16 July 2015
ICSV22
The 22nd International Congress on Sound and Vibration

THERMO-ACOUSTIC CHARACTERIZATION OF A HEAT EXCHANGER IN CROSS FLOW USING COMPRESSIBLE AND WEAKLY COMPRESSIBLE NUMERICAL SIMULATION

Strobio Chen Lin, Witte Armin, Polifke Wolfgang
Professur für Thermofluiddynamik, TU München, D-85747, Garching, Germany
email: strobio@tfd.mw.tum.de

In the present work, a heat exchanger as used for hot water supply in domestic boilers is investigated numerically. The objective of the study is to identify the frequency response of the heat transfer rate with respect to perturbations of flow velocity, and the acoustic scattering matrix of the heat exchanger. These response functions are determined by CFD simulation of flow with heat transfer combined with system identification. Unsteadiness is imposed on the simulations by broad-band excitation of the variables at the boundaries. The resulting time series are post-processed to obtain the frequency responses. Particular emphasis is placed on the comparability between compressible and weakly compressible simulations in terms of heat release response. The response functions may be used subsequently in thermo-acoustic stability analysis of combustion systems.

1. Introduction

The presence of heat exchangers in industrial applications is ubiquitous. Tthey can be found in most energy conversion systems, and are used in both cooling (industrial turbines, internal combustion engines) and hot water production systems (domestic heating, industrial boilers). Despite the wide range of applications, little is known about the thermo-acoustic scattering properties of heat exchangers, and about their role in system stability. This is due to the fact that heat exchangers are classified as heat sinks, which are often erroneously regarded as damping elements. Indeed, according to the Rayleigh criterion, instability may occur whenever the global Rayleigh index (evaluated in the volume of heat release V) is positive over an oscillation cycle of period T [10]:

$$G = \int_V \frac{1}{T} \int_T \dot{q}'(x,t) p'(x,t) \mathrm{d}t \, \mathrm{d}v > 0, \tag{1}$$

where $\dot{q}'(x,t)$ is the heat release rate fluctuation per unit volume and $p'(x,t)$ is the fluctuation in pressure. This means that, in presence of acoustics, a heat sink might either damp or drive system instability, depending on the phase between the heat release fluctuations and the pressure field. In the present work, a typical configuration of heat exchanger employed in domestic boilers (Fig. 2) is investigated numerically. The aim is to characterize the behavior of the heat exchanger in terms of its acoustic scattering matrix and its heat release response to upstream acoustic perturbations. The

results of the identification can subsequently be used as input for an acoustic network model, in order to perform stability analysis.
The choice of a numerical approach is justified by the fact that in experimental test rigs, it is very difficult to measure the local instantaneous heat release rate. However, fully resolving the acoustics leads to very high computational costs. Therefore, in presence of low Mach and Helmholtz numbers, it is more convenient to treat the flow as incompressible [3],[6]. For compact heat sources ($He \ll 1$), in which the geometrical length is much smaller than the acoustic wavelength, the incompressible-flow approximation has some advantages: it is, in fact, computationally less expensive, and no acoustic reflections occur at the boundaries. Yet, in this specific case, the compactness is not always satisfied, since the Helmholtz number is in the range of $He \in [0, 0.5]$ (see Section 2.2.1). For this reason, is necessary to compare the incompressible simulation to a fully compressible case, in order to validate or discuss possible discrepancies. In the present study, since heat transfer takes place, a "weakly compressible" solver is proposed (see Section 2), which allows for changes in density depending solely on temperature.
In section 2, the details of the simulation and system identification procedure are given for both compressible and incompressible cases. In section 3, the results in terms of heat release fluctuations will be discussed. In section 4, an analytical modeling of the heat exchanger element has been carried out, in order to shed light on the physical phenomena governing the acoustic scattering of the heat exchanger. The results are discussed in terms of acoustic scattering matrix coefficients, and compared against the results from the fully compressible simulation, where direct identification of the scattering behavior is possible.

2. Numerical Approach

2.1 Compressible and weakly-compressible simulation

To create the time series necessary for system identification, CFD simulations were used. For the fully compressible simulations (FCS), the standard solver buoyantPimpleFoam, developed in OpenFOAM®, is used. buoyantPimpleFoam is apt for solving unsteady problems involving heat transfer and buoyancy effects. Neglecting the buoyancy effects, the local total pressure in buoyantPimpleFoam is expressed as:

$$p(t, x) = p_d(t, x) + p_\infty, \tag{2}$$

in which the instantaneous total pressure is a sum of the dynamic pressure (p_d) and of the constant reference pressure (p_∞).
The weakly compressible simulation (WCS), on the other hand, adopts a modified version of the original solver. The main modification concerns the relation density-pressure. In the WCS, the instantaneous pressure $p(t)$ is used for the transport equations, while the thermodynamic model follows an isobaric approach. The equation of state for a perfect gas is in fact changed to:

$$\rho(t, x) = \frac{p_\infty}{R\,T(t, x)}, \tag{3}$$

where R is the gas constant, T is the instantaneous temperature. p_∞ is not the instantaneous pressure, but constant over time. Hence, density variations depend solely on temperature variations.

2.2 Simulation domain and boundary conditions

2.2.1 General numerical details

In most hot water production systems, the heat exchanger (HX) and the hot gases are in a cross-flow configuration. The hot gases flow through a row of cylinders and heat is transferred to the water

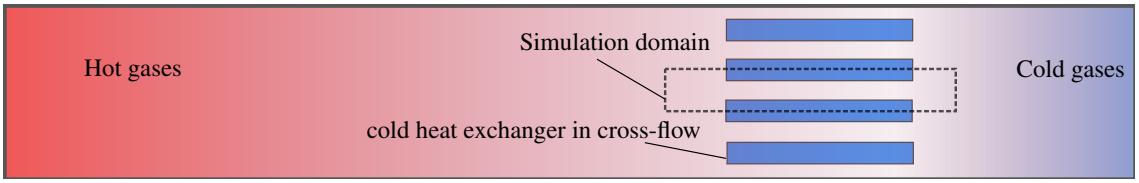

Figure 1. The geometry of a combustion system with row of HX cylinders in cross-flow

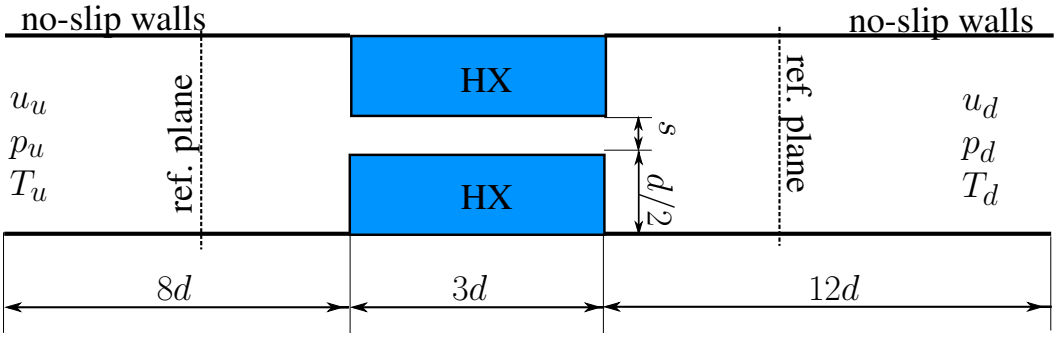

Figure 2. The geometry of the domain. The blue region represents the HX filled with water at constant temperature $T_{HX} = 300K$. The figure is not drawn to scale.

(see Fig. 1). In most applications, in order to optimize the heat exchange process, the surface of the cylinders is maximized with respect to the volume, therefore the cross section of the tubes are not circular, but elongated. In this study, we consider a simple 2D model (see Fig. 2), with two rectangular half tubes inside a channel. The height of the narrow channel between the tubes is $s = 0.8\,[mm]$, while the diameter of the HX tube is $d = 12.8\,[mm]$. This domain represents a single portion of the periodic configuration in Fig. 1. For the upper and lower boundaries, an adiabatic, no-slip wall condition is adopted instead of the cyclic boundary condition, in order to stabilize the downstream flow, which shows relevant transversal velocity components after the sudden area expansion. The velocity of the hot gases at the inlet is $\bar{u}_u = 0.89\,[m/s]$, which corresponds to a Mach number of $M_u = 1.28 \cdot 10^{-3}$. The maximum velocity is reached at the beginning of the narrow channel, $\bar{u}_{max} \approx 12\,[m/s]$. At the outlet, a constant pressure boundary condition has been set to $\bar{p}_d = 100\,[kPa]$. The temperature at the inlet is imposed at $\bar{T}_u = 1200\,[K]$, while the temperature at the heat exchanger is assumed to be constant $\bar{T}_{HX} = 300\,[K]$. The constant temperature assumption simplifies the analysis. However, the 'oversized' cooling in the HX implies that the temperature at the exit, $\bar{T}_d = 320\,[K]$, is lower than in the real case. The flow regime is laminar, since the highest Reynolds number in the domain is $Re_{max} = 180$.
Taking the upstream speed of sound as reference value, the Helmholtz number ($He = \omega L_{HX}/\bar{c}_u$) ranges from 0 to 0.45 for frequency range between 0 and 1500 Hz. A grid independence study has been carried out, in order to determine the level of refinement in the HX channel which properly resolves the boundary layer, where most of the heat exchange takes place. As a result, the channel height (s) has been divided into 16 squared cells.

2.2.2 *Fully compressible simulation*

In the fully compressible simulation the propagation of sound waves has to be resolved. The largest time step which allows to resolve the acoustic propagation properly is $\Delta t_{max} = \frac{Co_{max} \cdot \Delta x_{min}}{\bar{u}_u + \bar{c}_u} \approx 7 \cdot 10^{-8}\,[s]$, in which Co_{max} equals unity, according to the Courant-Friedrichs-Lewy condition.
The time step used in the simulation is $\Delta t_{fcs} = 5 \cdot 10^{-8}\,[s]$, which corresponds to a maximum Courant number of $Co_{max} = 0.7$.

Because of the presence of acoustically reflecting boundary conditions, the steady state solution was obtained by applying the Navier-Stokes Characteristic Boundary Conditions (NSCBCs) [8] at inlet and outlet. These boundary conditions ensure an exponential decay (w.r.t. frequency) of the reflection coefficient at the boundaries. However, partial reflection is still present at lower frequencies.

2.2.3 Weakly compressible simulation

Concerning the weakly compressible simulation, the considerations on the mesh refinement and initial conditions ($\bar{u}$, $\bar{p}$, $\bar{T}$) are unchanged. However, since there is no propagation of acoustic waves in the domain, no manipulations are needed for the inlet and outlet boundary conditions. Moreover, the time step adopted ($\Delta t_{wcs} = 2 \cdot 10^{-6}\,[s]$) has only to satisfy the fluid-dynamic CFL number and is roughly two orders of magnitude larger than the Δt_{fcs}. This makes the WCS suitable for generation of long time series (in the order of seconds), which is useful in the identification of the acoustic response at low frequencies.

2.3 System excitation and identification

The behavior of a system in presence of acoustic disturbances is characterized by its heat release response to upstream velocity perturbations $\mathcal{F}(\omega)$:

$$\mathcal{F}(\omega) = \frac{\dot{Q}'(\omega)/\bar{\dot{Q}}}{u'_u(\omega)/\bar{u}_u}, \tag{4}$$

where $\dot{Q}'$ is the fluctuation in heat release rate of the heat exchanger and u'_u is the velocity probe at the reference plane (see Fig. 2); and by its acoustic scattering matrix:

$$\begin{pmatrix} f_d \\ g_u \end{pmatrix} = \begin{bmatrix} T_{u\to d} & R_d \\ R_u & T_{d\to u} \end{bmatrix} \begin{pmatrix} f_u \\ g_d \end{pmatrix}, \tag{5}$$

where f and g are, respectively, the waves propagating in downstream and upstream direction. They are related to the acoustic perturbations (p',u') as follows:

$$f = \frac{1}{2}\left(\frac{p'}{\bar{\rho}\bar{c}} + u'\right) \qquad g = \frac{1}{2}\left(\frac{p'}{\bar{\rho}\bar{c}} - u'\right). \tag{6}$$

For the identification of the heat release response $\mathcal{F}(\omega)$ in the FCS, a Single-Input Single-Output (SISO) approach is adopted. After imposing an excitation signal (f) at the inlet, the model is identified by considering the upstream velocity fluctuations as the input and the fluctuations in the instantaneous total heat release as the output. As for the scattering matrix, a Multi-Input Multi-Output (MIMO) approach is used, in which excitation signals (f_u, g_d) are applied respectively at the inlet and outlet, and the outputs (f_d, g_u) are measured at the reference planes (see Fig. 2). The wavelet-based excitation signals present a constant power spectral density in the frequency range under investigation ($f \in [0; 1500]$ Hz) and are statistically uncorrelated [1]. The identification of the models from the time series is performed with the Box-Jenkins parametric model structure [7], in order to handle the noise deriving from the NSCBC partially reflecting boundaries. In the WCS a similar identification process is pursued. However, the excitation signals imposed correspond to u' at the inlet in the SISO approach and to u' and p' respectively at inlet and outlet in the MIMO approach. This is because, in an incompressible simulation, all disturbances travel at infinite speed and no acoustic wave (as f and g) can propagate across the domain.

3. Results from Compressible and Weakly Compressible Simulations

In this section, the frequency response from the FCS and WCS are compared. Before analyzing the results, it is necessary to point out that the time series of the two simulations are not immediately

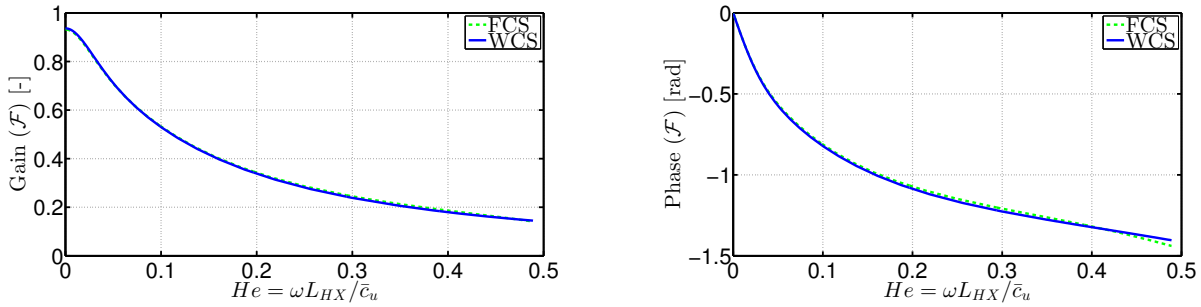

Figure 3. Gain and phase of the HX transfer function for compressible (green-dashed line) and weakly-compressible (blue line) simulations

comparable. In fact, in the compressible simulation, the signals of $u'/\bar{u}$ vary according to the position of the reference plane, since they are non-causal and derive from the superposition of the Riemann invariants f and g at the reference plane. In order to make the velocity signal space-invariant, it is necessary to first manipulate the Riemann invariants of the reference plane, by shifting them to the position of the heat exchanger. Since f and g travel in opposite directions, the time series of f is shifted forward, while g is shifted backwards for the upstream velocity. The time associated to the shift for f is: $\tau(f) = \Delta x/(\bar{c} + \bar{u})$, while for g is: $\tau(g) = \Delta x/(\bar{c} - \bar{u})$, where Δx is the distance between the reference plane and the HX and $\bar{c}$ and $\bar{u}$ are the mean speed of sound and flow velocity, respectively. Being the shifted time series f^* and g^*, it is possible to reconstruct the space-invariant velocity signal as $u'^* = f^* - g^*$. The heat exchanger transfer function for the compressible simulation is therefore expressed as in Eq. (4), with u'^* as fluctuating velocity.

3.1 Frequency response of heat transfer

Given the quasi-steady approximation used in the WCS, differences in gain and phase are expected for higher frequencies. However, the results in Fig 3 do not show any substantial difference between the transfer functions. Slight departures show at $He = 0.2$, but the difference in both gain and phase are negligible. This means that the weakly compressible simulation can capture with a good approximation all the fluid-dynamic features of the system, such as heat release and the changes in the velocity field, up to the frequency range considered ($f \in [0, 1500]Hz$). Significant difference only shows in the phase startin from $He \approx 0.48$.

3.2 Low frequency limit of the heat release response

The transfer function of the HX shows a low-pass filter behavior. Such behavior is common in the transfer functions of most heat sources, particularly in flames. However, as argued in [9] and experimentally demonstrated in [5], the zero-frequency limit of the transfer function in perfectly premixed flames should equal unity. Here, the low frequency limit of the heat exchanger transfer function is lower than 1. In order to explain such difference, it is necessary to analyze the physics involved in the heat exchanger. In [9] it is shown how the response of heat sources in the low-frequency limit can be derived from global conservation equations in quasi steady state.
The enthalpy balance for the HX is:

$$\dot{Q} = \dot{m}\Delta h = A_{\text{flow}} u_u \rho_u c_p (T_u - T_d), \tag{7}$$

where A_{flow} is the cross section of the channel, $u_u\rho_u$ is the mass flow rate and $c_p(T_u - T_d)$ is the specific enthalpy transferred from the hot gases to the HX. Considering that, in presence of low Mach numbers and acoustic disturbances only, the normalized density fluctuation is negligible w.r.t. the

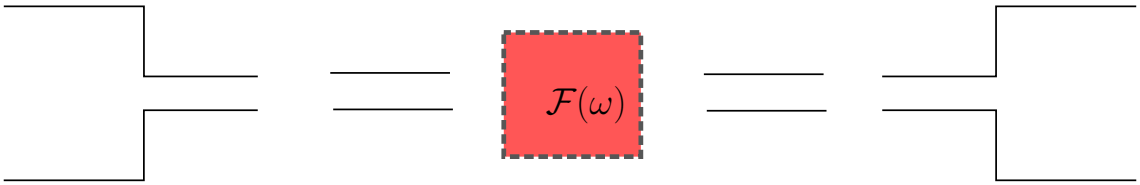

Figure 4. Acoustic model of the heat exchanger as: area change - duct - heat sink - duct - area change

velocity fluctuations, we have for the transfer function

$$\lim_{\omega\to 0}\mathcal{F} = \frac{\dot{Q}'/\overline{\dot{Q}}}{u'_u/\overline{u}_u} = 1 - \left(\frac{T'_d}{\overline{T}_u - \overline{T}_d}\Big/\frac{u'_u}{\bar{u}_u}\right). \tag{8}$$

Eq. (8) shows that the transfer function of the HX is lower than unity, whenever the fluctuation in downstream temperature is positive. In order to correlate the downstream temperature fluctuation T'_d to the velocity fluctuation u'_u, we consider the local temperature function in a simple 2D channel geometry:

$$T_d = T_{\mathrm{HX}} + (T_u - T_{\mathrm{HX}})\exp\left(\frac{-\mathrm{Nu}_\infty \lambda L}{2\rho_u u_u s^2 c_p}\right). \tag{9}$$

Assuming that fluctuations in temperature are only caused by velocity fluctuations, it may be argued that T'_d can be approximated as $T'_d(u'_u) \approx \frac{d\bar{T}_d}{d\bar{u}_u}u'_u$, which gives for the low frequency limit of $\mathcal{F}$:

$$\lim_{\omega\to 0}\mathcal{F} = 1 - \frac{\bar{T}_u - T_{\mathrm{HX}}}{\bar{T}_u - \bar{T}_d}\frac{\mathrm{Nu}_\infty \lambda L}{2\bar{\rho}_u \overline{u}_u s^2 c_p}\exp\left(\frac{-\mathrm{Nu}_\infty \lambda L}{2\bar{\rho}_u \overline{u}_u s^2 c_p}\right). \tag{10}$$

Eq. (10) shows that the lower frequency limit of the transfer function differs from unity, except from some limit cases, in which the product on the r.h.s is zero. This condition is verified for two cases: $L \to \infty$ and $s \to 0$. The first limit case shows that only when a heat exchanger has infinite surface, the downstream temperature fluctuation is zero. In the second case, the height of the channel is infinitesimally small, so the heat exchange takes place instantaneously via heat conduction. In real applications, neither of the cases cited above is verified. Therefore, the zero frequency limit of the heat exchanger transfer function is generally below unity.
There are no exact analytical relations for the geometry of the HX under analysis, so no quantitative values of $\lim_{\omega\to 0}\mathcal{F}$ can be given for comparison. However, regardless of the geometry, the qualitative considerations given above are valid for any heat source (or sink) in which heat exchange is involved.

4. System Modeling

As previous works have shown [1], the fully compressible simulation, combined with system identification can give very reliable results in terms of acoustic scattering matrix and heat release response. The results obtained for scattering matrix from the identification are shown in Fig. 5 (green line). Fully resolving the acoustic propagation is, however, more expensive in terms of computation efforts compared to the WCS. In this section, we will try to reproduce the scattering behavior identified with the FCS, using the results for the heat exchange rate obtained from the WCS. This modeling process not only gives insight into the scattering process at the HX, but would also enable the use of the incompressible simulation for describing acoustics of non-compact elements. In this attempt, we have modeled the system in Fig. 2 as a network of basic elements, as depicted in Fig. 4: As shown in Fig. 4, the heat exchanger is represented with all its geometric features, while the heat release is concentrated at the center of the network. This choice is justified by the fact that, for a reasonably high range of frequencies ($f \in [0, 1500]\,Hz$), the weakly compressible transfer function still gives a

good approximation of the heat transfer dynamics. Therefore, the heat source can still be considered as compact, at low Helmholtz numbers. The transfer functions in terms of $\frac{p'}{\bar{\rho}\bar{c}}$ and u' for the area change (ac) and the duct are:

(11)

$$TM_{ac} = \begin{bmatrix} 1 & -i\omega L_{eff}/\bar{c} \\ i\omega L_{red}/\bar{c} & \alpha \end{bmatrix}, \qquad TM_{duct} = \frac{1}{2}\begin{bmatrix} \left(e^{ik^- L} + e^{-ik^+ L}\right) & \left(-e^{ik^- L} + e^{-ik^+ L}\right) \\ \left(-e^{ik^- L} + e^{-ik^+ L}\right) & \left(e^{ik^- L} + e^{-ik^+ L}\right) \end{bmatrix},$$

where $L_{eff} = 0.0064\,[m]$ and L_{red} are end correction coefficients, which depend on the ratio between the cross-sections (α); as shown in [2], the value of L_{red} is negligible. In the transfer matrix of the duct L is the length of the channel and $k^{\pm} = \frac{\omega}{\bar{c}\pm\bar{u}}$. Considering the Rankine-Hugoniot relations for thermoacoustics [4], the transfer matrix across a concentrated heat source is:

(12)
$$TM_{pu,RH} = \begin{bmatrix} \frac{\bar{\rho}_u \bar{c}_u}{\bar{\rho}_d \bar{c}_d} & -\frac{\bar{\rho}_u \bar{c}_u}{\bar{\rho}_d \bar{c}_d}\left(\frac{T_d}{T_u} - 1\right) M_u(1 + \mathcal{F}(\omega)) \\ -\left(\frac{T_d}{T_u}\right)\gamma M_u & 1 + \left(\frac{T_d}{T_u} - 1\right)\mathcal{F}(\omega) \end{bmatrix}.$$

It consists of a 'semi-analytical' approach, since well-known analytical models are employed together with the transfer function $\mathcal{F}(\omega)$ given by the numerical simulation. The total transfer matrix in terms of $p'/\bar{\rho}\bar{c}$ and u' will be given by the product of the transfer matrices of the single elements. The results are shown in Fig. 5 in terms of the scattering matrix (see Eq. (5)), which is obtained from an algebraic manipulation of the transfer matrix. In Fig. 5, the model (blue line) is compared against the scattering matrix identified numerically (green-dashed line). Significant discrepancies are found in the transmission coefficients up and down stream and minor discrepancies in the low frequency region for the other terms. This means that the approximation of a concentrated heat release does not represent the heat exchanger very well. In fact, the model is qualitatively wrong, even if all the main qualitative features are present. Several hypothesis can be made to explain the discrepancies. First, the heat release is not equally distributed along the HX, but occurs for the most part at the front stagnation point and at the beginning of the duct, where the temperature gradient is higher. In addition, the presence of heat release at the front stagnation point might influence the scattering properties of the area change. Moreover, the sudden expansion downstream could also cause acoustic dissipation, due to the presence of sharp edges.

5. Conclusion

In this work, the identification of the transfer function and scattering matrix of a cold heat exchanger in hot cross flow is presented. The objective is not only to obtain a validated model for stability studies, but also to validate the effectiveness of the weakly compressible solver in handling acoustic simulation. The results show that the weakly compressible solver is apt for identifying the leading order effects, such as heat release and velocity fluctuaitons for a wide range of frequencies. At higher frequencies some discrepancies arise. However, such discrepancies do not have much influence, since the gain is close to zero. An attempt to model the HX analytically has been made. Comparison to results from direct identification shows that the approach used in the modeling is not satisfactory. To fully understand the mechanisms of acoustic scattering in a heat exchanger, further studies are needed on the behavior of the single acoustic elements (channel, area change) in presence of heat release.

6. Acknowledgements

The presented work is part of the Marie Curie Initial Training Network Thermo-acoustic and aero-acoustic nonlinearities in green combustors with orifice structures (TANGO). We gratefully acknowledge the financial support from the European Commission under call FP7-PEOPLE-ITN-2012.

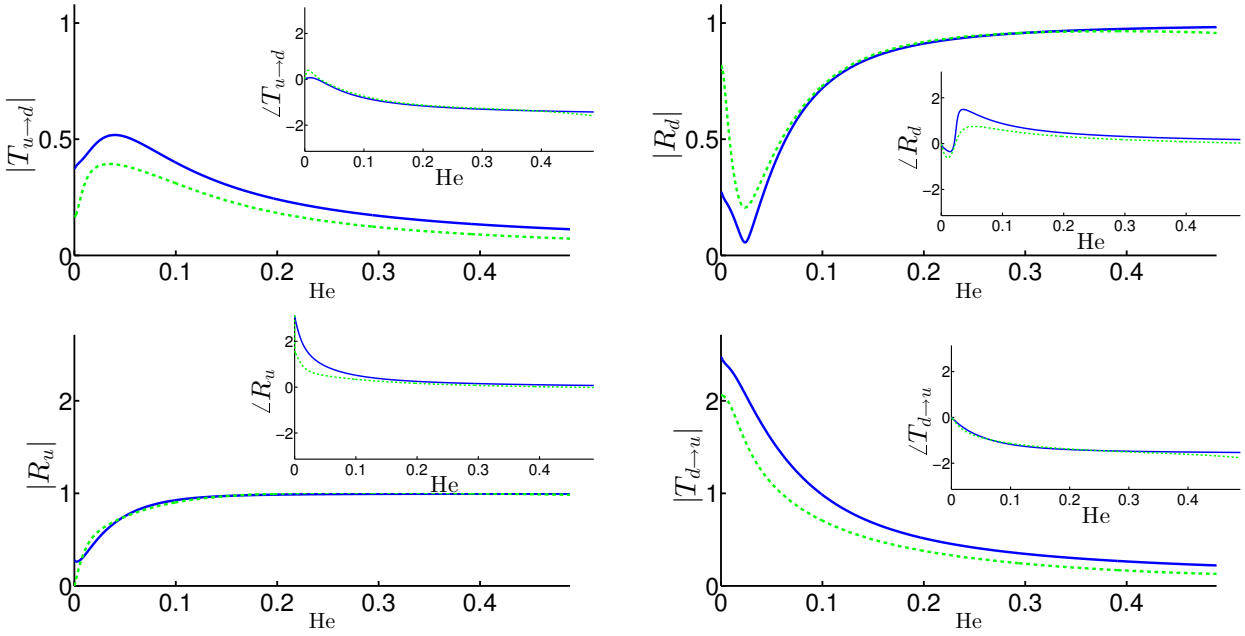

Figure 5. Scattering matrix amplitude (main frames) and phase (insets) for FCS (green-dashed line) and network model (blue line)

Financial support for Armin Witte by the German Research Foundation DFG, project PO 710/15-1 and the Technische Universität München are gratefully acknowledged.

REFERENCES

1. Polifke W Foeller S. Identification of aero-acoustic scattering matrices from large eddy simulation. Application to a sudden area expansion of a duct. *Journal of sound and vibration*, 331(13):3096–3113, 2012.
2. A. Gentemann, A. Fischer, S. Evesque, and W. Polifke. Acoustic transfer matrix reconstruction and analysis for ducts with sudden change of area. In *9th AIAA/CEAS Aeroacoustics Conference and Exhibit*, number AIAA-2003-3142, page 11, Hilton Head, SC, USA, May 2003. AIAA.
3. M. Karlsson and M. Abom. Quasi-steady model of the acoustic scattering properties of a T-junction. *Journal of Sound and Vibration*, 330(21):5131–5137, 2011.
4. J. J Keller. Thermoacoustic oscillations in combustion chambers of gas turbines. *AIAA Journal*, volume 33, number 12:2280–2287, 1995.
5. Kornilov V.N., Rook R., ten Thije Boonkkamp JHM, and de Goey LPH. Experimental and numerical investigation of the acoustic response of multi-slit bunsen burners. *Combustion and Flame*, 156(10):1957–1970, 2009.
6. Lacombe R., Moussou P., and Auregan Y. Identification of whistling ability of a single hole orifice from an incompressible flow simulation. In *ASME 2011 Pressure Vessels and Piping Conference*, pages 261–267. American Society of Mechanical Engineers, 2011.
7. L. Ljung. *System Identification - theory for user*. Prentice Hall, 1999.
8. W. Polifke, C. Wall, and P. Moin. Partially reflecting and non-reflecting boundary conditions for simulation of compressible viscous flow. *J. of Comp. Physics*, 213:437–449, 2006.
9. Polifke Wolfgang and Lawn Chris. On the low-frequency limit of flame transfer functions. *Combustion and flame*, 151(3):437–451, 2007.
10. Lord Rayleigh. *The theory of sound*. Number Rayleigh. Macmillan, 1896.